# Rethinking Memory in Continual Learning: Beyond a Monolithic Store of the Past

**Anonymous authors**
**Paper under double-blind review**

## Abstract

Memory is a critical component in replay-based continual learning (CL). Prior research has largely treated CL memory as a monolithic store of past data, focusing on how to select and store representative past examples. However, this perspective overlooks the higher-level memory architecture that governs the interaction between old and new data. In this work, we identify and characterize a dual-memory system that is inherently present in both online and offline CL settings. This system comprises: a short-term memory, which temporarily buffers recent data for immediate model updates, and a long-term memory, which maintains a carefully curated subset of past experiences for future replay and consolidation. We propose *memory capacity ratio* (MCR), the ratio between short-term memory and long-term memory capacities, to characterize online and offline CL. Based on this framework, we systematically investigate how MCR influences generalization, stability, and plasticity. Across diverse CL settings—class-incremental, task-incremental, and domain-incremental—and multiple data modalities (e.g., image and text classification), we observe that a smaller MCR, characteristic of online CL, can yield comparable or even superior performance relative to a larger one, characteristic of offline CL, when both are evaluated under equivalent computational and data storage budgets. This advantage holds consistently across several state-of-the-art replay strategies, such as ER, DER, and SCR. Theoretical analysis further reveals that a reduced MCR yields a better trade-off between stability and plasticity and lowers a bound on generalization error when learning from non-stationary data streams with limited memory. These findings offer new insights into the role of memory allocation in continual learning and underscore the underexplored potential of online CL approaches.[1]

## 1 Introduction

Deep neural networks are commonly trained by collecting a large dataset upfront to create independent and identically distributed (IID) mini-batches that are used to optimize network parameters using stochastic gradient descent (SGD). When learning from non-IID data where new tasks need to be learned over time as data for these tasks becomes available, these networks often suffer from catastrophic forgetting, where new information overwrites what has been learned previously. Algorithms for continual learning (CL) aim to address this by enabling the acquisition of new skills and knowledge with minimum impact on what has been learned in the past. Two primary problem settings are considered in this context: offline CL and online CL. Offline CL assumes that when a new task needs to be learned, a new training dataset becomes available from which IID mini-batches can be drawn. In contrast, in online CL, a stream of mini-batches is presented to the algorithm without any side information.

A major challenge in both online and offline CL is balancing the acquisition of new knowledge, referred to as "plasticity', with the retention of previous knowledge, known as "stability", especially when resources like memory and computation are limited. Replay-based methods, which maintain a subset of past samples, often called exemplars, to adjust gradients during optimization, have shown promise in mitigating forgetting and achieved state-of-the-art CL performance. However, previous studies that applied these methods in online

[1]Code: https://anonymous.4open.science/r/long-term-short-term-2CBD

CL Mai et al. (2022); Soutif-Cormerais et al. (2023) often report lower performance compared to studies that applied the same methods in offline CL Masana et al. (2022); Buzzega et al. (2020). This suggests online continual learning is inherently more difficult. Specifically, the issue of potentially insufficient plasticity has been highlighted in (Zhang et al., 2022; Jung et al., 2022): without the ability to store the entire data representing a new thing to be learned and training for multiple epochs on this data, online methods are prone to underfitting.

In this paper, we challenge this notion by showing that the limitations in performance seen in online CL are primarily due to constrained memory and computing resources rather than the online setting itself. Perhaps more interestingly, we show that, depending on the replay mechanism used, online CL can achieve greater plasticity than offline CL. For instance, we demonstrate that the online version of DER++ (Buzzega et al., 2020) exhibits greater plasticity than its offline counterpart. More specifically, we provide a controlled comparison between online and offline CL by accounting for disparities in compute and memory budgets and introduce the "memory capacity ratio" (MCR) to represent the relative sizes of short-and long-term memory. Here, short-term memory refers to the storage space available to store new data and long-term memory represents the capacity available to store past data. We demonstrate that the fundamental distinction between online and offline CL lies in their MCRs: online CL operates with a smaller short-term memory equal to the size of incoming streaming batch size, while offline CL utilizes a larger one equal to the size of task data (see Algorithm 1). Since the short-term memory contains new information that the model has not encountered, and long-term memory stores previously learned information that has been repeatedly trained, the capacity ratio between these two memory types is closely related to the stability and plasticity of continual learning systems. We systematically investigate two fundamental open questions: "*How does the MCR affect stability, plasticity, and generalization in experience replay?*" and "*How does the effect of the MCR interact with forgetting mitigation strategies (e.g., contrastive replay or knowledge distillation regularization) and the characteristics of the learning problem (e.g., whether it is class incremental, domain incremental or task incremental)?*".

**Algorithm 1:** Unified continual replay framework instantiated with experience replay

// Non-stationary data stream: $\mathcal{D}_t = \cup_t \mathcal{X}_t$, where $\mathcal{X}_t$ is the incoming batch
// Short-term memory $\mathcal{M}_{short}$: storing new data
// Long-term memory $\mathcal{M}_{long}$: storing past data
// offline CL: $|\mathcal{M}_{short}|$ is equal to the task size $|\cup_{T_i \leq t < T_{i+1}} \mathcal{X}_t|$
// online CL: $|\mathcal{M}_{short}|$ is equal to the stream batch size $|\mathcal{X}_t|$
// The memory management policy $\pi$ selects samples from $\mathcal{M}_{short}$ for storage in $\mathcal{M}_{long}$.

```
function ContinualLearning(X_t, θ, M_short, M_long,)
    M_short ← M_short ∪ X_t // Update short-term memory
    if M_short is full then
        θ ← ModelTraining(θ, M_short, M_long)
        M_long ⊂_π M_short ∪ M_long // Update long-term memory
        M_short ← ∅
    return θ, M_short, M_long
function ModelTraining(θ, M_short, M_long)
    for K epochs do
        for B_short in M_short do
            sample B_long from M_long,
            θ ← θ − η∇L(B_short ∪ B_long; θ) // Using basic experience replay as an example
    return θ
```

We conduct a theoretical analysis based on a bound on the generalization error in a simplified setting with 0-1 classification loss showing that 1) the effect of the MCR depends on task similarity and problem structure; 2) a small MCR can lead to a lower bound under certain conditions (Section 4). Subsequently, we investigate whether this theoretical result can be extended to practical CL algorithms with various complex forgetting

mitigation strategies. We empirically study the effect of MCR by controlling the memory budget, training data, forgetting mitigation strategies, and training regimes. The generalization performance of continual learning is measured by the accuracy of a separate test set representing all the information to be learned. Across four state-of-the-art replay strategies, we observe that a smaller MCR leads to comparable or superior performance compared to a larger MCR value.

Contrary to conventional wisdom, we show that online CL, with a smaller MCR, does not necessarily compromise plasticity compared to offline approaches. Our analysis reveals that, depending on the replay mechanism and regularization design employed, reducing the MCR can lead to three types of changes in stability and plasticity: a) improved stability at the cost of reduced plasticity, b) enhanced plasticity with reduced stability, or c) simultaneous improvements in both stability and plasticity (Section 6). Overall, our work provides new insights into memory allocation dynamics in continual learning and highlights the potential of online CL to achieve superior performance particularly in environments where memory and computational resources are constrained.

## 2 Related work

**Continual learning**. General continual learning (Delange et al., 2021; Buzzega et al., 2020) is an idealized scheme for learning from an infinite data stream, with desiderata like constant memory, online learning, no task boundaries, no task labels, and graceful forgetting. Various relaxations exist with different assumptions. Early work focused on so-called "task-incremental" settings (Mallya & Lazebnik, 2018; Serra et al., 2018) that assume access to task labels during training/testing. Despite promising results, relying on a task oracle is impractical. Recent so-called "class-incremental" and "domain-incremental" learning approaches remove this assumption (Mirza et al., 2022; Masana et al., 2022; Van de Ven & Tolias, 2019). Nevertheless, these methods still require the knowledge of task boundaries to allow multi-epoch training over tasks. In contrast, online continual learning (Chaudhry et al., 2019; Aljundi et al., 2019; Mai et al., 2022) does not collect a specific task dataset but rather trains the model incrementally as mini-batches of new data become available.

**Memory and compute**. In the literature, online and offline continual learning are studied separately with different memory and computational setups (see Table B in the Appendix B). Studies and surveys of offline continual learning usually utilize 50-250 training epochs per task on standard benchmarks. Online continual learning, by design, can only use a single "epoch", but the number of gradient update steps can be increased through repeated iterations yielding multiple gradient-based updates for each incoming batch (Zhang et al., 2022; Soutif-Cormerais et al., 2023). However, it is common practice to limit the number of iterations to fewer than 10, potentially putting online learning at a disadvantage. Considering storage costs, a common practice in continual learning is to compare different online or offline methods based on a fixed budget for storing exemplars—a subset of past samples. This approach views memory in continual learning as a single system comprised solely of exemplars. In contrast, we consider the actual amount of data that needs to be stored, comprising both short-term and long-term memory. By controlling the total storage required to hold data—referred to as memory—and the number of iterations yielding gradients, we examine the effect of relative capacity of long-term and short-term memory on learning efficacy.

**Theoretical study in continual learning**. There are several theoretical studies deriving bounds on generalization performance for continual learning. (Peng et al., 2023; Doan et al., 2021) provide theoretical analysis with PAC-Bayes bounds. Ye & Bors (2022) derives a bound for 0-1 loss based on discrepancy distance and Rademacher complexity, similar to our work but only considers the effect of exemplars in the analysis. Here, we consider the samples in both long-term and short-term memory.

## 3 Rethinking CL memory: beyond a monolithic store of past data

### 3.1 Problem setup

In this paper, we consider the general continual learning problem proposed in Delange et al. (2021), which deals with infinite non-stationary data streams. We study this problem with a unified continual replay framework.

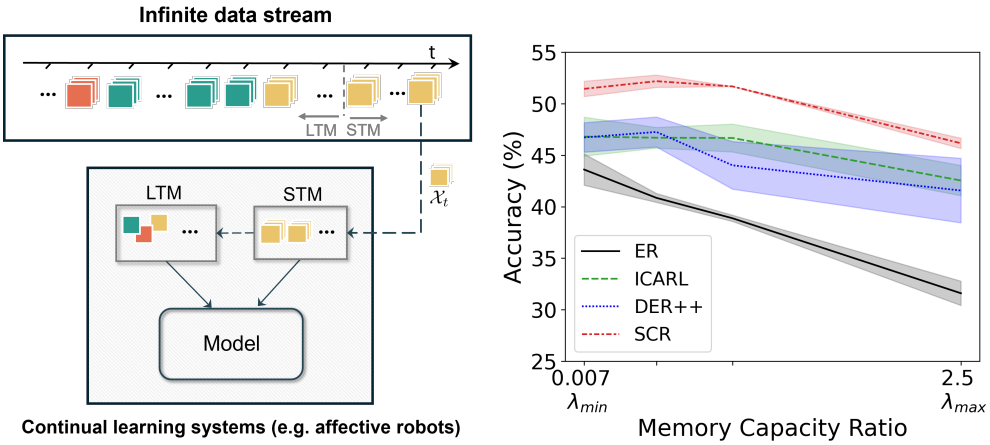


(a) (b)

Figure 1: Long-term and short-term memory structure in continual replay: (a) The short-term memory (STM) greedily stores the incoming data and the long-term memory (LTM) selectively stores a subset of data after model training. (b) The effect of the memory capacity ratio (MCR=STM/LTM): reducing MCR significantly boosts the learning efficacy of continual learning algorithms including ER, iCARL, DER++, SCR on Split-Mini-ImageNet.

**Non-stationary data stream**. At each time step $t$, a continual learning algorithm $\mathcal{A}$ receives an incoming batch of data samples of size $B$, $\mathcal{X}_t = \{\mathbf{x}_i, y_i\}_{i=1,..,B}$, drawn from the current data distribution $\mathbb{P}_t$. Each batch forms part of a non-stationary (potentially infinite) stream of data $\mathcal{D}_t = \cup_t \mathcal{X}_t$. The distribution $\mathbb{P}_t$ may change at any time. A basic approach to continual learning from such a stream of data would be to attempt to minimize the empirical risk on all the data seen so far:

$$\min_{\theta} \mathcal{R}_t(\theta) = \min_{\theta} L(\cup_t \mathcal{X}_t; \theta). \tag{1}$$

with a loss function $L$, a CL network function $f : x \to y$, and its associated parameters $\theta$.

*Task boundaries.* The period where the data distribution $\mathcal{P}_t$ stays the same is often called a *task*. Task boundaries are defined as the time steps where changes in the data distribution occur, i.e., $\{T_i\} \doteq [t|\mathbb{P}_t \neq \mathbb{P}_{t-1}]$. Given the task boundaries of a data stream, each task data can be denoted as $\mathcal{C}_i = \cup_{T_i \leq t < T_{i+1}} \mathcal{X}_t$ and $\cup_i \mathcal{C}_i = \mathcal{D}_t$.

### 3.2 Proposed unified dual-memory structure

Although prior works often treat the CL memory as a monolithic store of past data and focus on strategies for managing these past exemplars, we argue that a higher-level memory structure governs the interaction between new and old data in continual learning. We show that a dual-memory system, comprising short-term and long-term memory, naturally arises in both online and offline CL, as illustrated in Figure 1. Moreover, we identify the memory capacity ratio (MCR) as a key factor influencing the efficiency of this memory system.

We formalize this with a Unified Continual Replay framework $UCR(M_s, M)$: Given a total data storage budget $M$ ($M < |\mathcal{D}_t|$) and a stream of data $\mathcal{D}_t = \cup_t \mathcal{X}_t$ with batch size $B$, the storage space is divided into two parts: a short-term memory of size $M^t_{short}$ ($M_s \geq B$) and a long-term memory of size $M - M_{short}$. The short-term memory $\mathcal{M}^t_{short}$ greedily stores recent batches from the data stream until it is full: $\mathcal{M}^t_{short} = \cup_{t-n+1,...,t} \mathcal{X}_t, n = \frac{M_{short}}{B}$. Each model training session begins when $\mathcal{M}^t_{short}$ is full. After the model training session, $\mathcal{M}^t_{short}$ is emptied, with some of the short-term memory samples moved into $\mathcal{M}^t_{long}$ based on some sample selection policy $\pi$: $\mathcal{M}^{t+1}_{long} \subset_{\pi} \mathcal{M}^t_{short} \cup \mathcal{M}^t_{long}$. This framework is agnostic to replay design. Algorithm 1 gives an example using Experience Replay with $K$ epochs.

Online and offline CL can be considered as two extreme cases of this framework. Offline CL stores the whole task data in short-term memory based on the knowledge of task boundaries: $M_{short} = |\cup_{T_i \leq t < T_{i+1}} \mathcal{X}_t| = C$. Online CL only stores the current batch in the short-term memory: $M_{short} = |\mathcal{X}_t| = B$.

**Memory Capacity Ratio**. We define the Memory Capacity Ratio as $\lambda = M_{short}/(M - M_{short})$. Offline CL yields a large value of MCR, i.e., $\lambda_{offline} = \lambda_{max} = C/(M - C)$, where $C$ is the task size, while online CL yields a small MCR: $\lambda_{online} = \lambda_{min} = B/(M - B)$, where $B$ is the streaming batch size.

*Semi-offline CL*. Apart from the two extreme cases, representing offline and online continual learning respectively, the unified framework enables investigation of a novel semi-offline setting, where the short-term memory stores more than one streaming batch, and $B < M_{small} < C$. We investigate what the optimal value for $\lambda$ is in $[\lambda_{min}, \lambda_{max}]$.

## 4 Theoretical study on generalization bound with 0-1 loss

To theoretically understand the effect of MCR on continual learning efficacy, we consider a bound on generalization error for 0-1 loss. To analyze generalization in a non-IID setting, we follow work on domain adaptation (Mansour et al., 2009) with 0-1 loss and derive a bound based on the concept of *discrepancy distance*.

**Definition 1** (Discrepancy distance). Mansour et al. (2009). Let $H$ be a set of functions mapping $X$ to $Y$ and let $L : Y \times Y \to R^+$ define a loss function over $Y$. The discrepancy distance between two distributions $Q_1$ and $Q_2$ over $X$ is defined by

$$\mathrm{disc}_L\left(Q_1, Q_2\right) \doteq \max_{h, h' \in H} \left|\mathcal{L}_{Q_1}\left(h', h\right) - \mathcal{L}_{Q_2}\left(h', h\right)\right|.$$

where the expected loss of two functions over a distribution is denoted as $\mathcal{L}_{\mathbb{Q}}(f, g) \doteq \mathrm{E}_{x \sim \mathbb{Q}}[L(f(x), g(x))]$.

We consider the stored data (i.e., data stored in the long-term and short-term memory) as the source domain, and the test data of the data stream as the target domain. Let $\mathbb{D}_t$ and $\mathbb{M}_t$ denote the true probability distributions of the data stream and the stored samples at time step $t$ respectively. Let $\hat{\mathbb{M}}_t$ denote the empirical distribution of stored samples with a finite sample size of $M$. The true labeling function of all the data seen so far is defined as $h_y^t$ [2]. Given the optimal solutions $h^*_{\mathbb{M}_t} \doteq \mathrm{argmin}_{h \in H} \mathcal{L}_{\mathbb{M}_t}\left(h, h_y^t\right)$ and $h^*_{\mathbb{D}_t} \doteq \mathrm{argmin}_{h \in H} \mathcal{L}_{\mathbb{D}}\left(h, h_y^t\right)$, the generalization bound is presented in Theorem 1[3].

**Theorem 1**. Let $H$ be a hypothesis set bounded by some $A_0 > 0$ for the loss function $L : L(h, h') \leq A_0$. For all $h, h' \in H$, assume that the loss function $L$ is symmetric and obeys the triangle inequality. Then, for any $h \in H$ and any $\delta > 0$, with probability at least $1 - \delta$, the following generalization bound holds:

$$\mathcal{L}_{\mathbb{D}_t}(h, h_y^t) \leq \mathcal{L}_{\hat{\mathbb{M}}_t}(h, h^*_{\mathbb{M}_t}) + \widehat{\Re}_{\mathcal{M}_t}(H) + 3A_0\sqrt{\frac{\log\frac{2}{\delta}}{2M}} + \mathrm{disc}_L(\mathbb{D}_t, \mathbb{M}_t) + \mathcal{L}_{\mathbb{D}_t}(h^*_{\mathbb{M}_t}, h^*_{\mathbb{D}_t}) + \mathcal{L}_{\mathbb{D}_t}(h^*_{\mathbb{D}_t}, h_y^t), \quad (2)$$

where $\widehat{\Re}_{\mathcal{M}}(H)$ is the empirical Rademacher complexity of the hypothesis set over the stored samples $\mathcal{M}_t = \mathcal{M}^t_{short} \cup \mathcal{M}^t_{long}$.

The proof follows derivations of Theorem 8 in Mansour et al. (2009) and Theorem 1 in Ye & Bors (2022) and is presented in Appendix A. Given the high expressivity of deep networks, $\mathcal{L}_{\mathbb{D}_t}(h^*_{\mathbb{D}_t}, h_y^t)$ approaches zero.

The memory management policy governs the relationship between the memory distribution ($\mathbb{M}_t$) and the data stream ($\mathbb{D}_t$). While Theorem 1 holds regardless of their similarity, the alignment between the two affects the tightness of the bound through the term $\mathcal{L}_{\mathbb{D}_t}(h^*_{\mathbb{M}_t}, h^*_{\mathbb{D}_t})$ on the right hand side of Theorem 1. Since $\mathbb{D}_t$

[2]Throughout this work, we assume the true labeling function $h_y^t$ is deterministic Ben-David & Urner (2014), i.e., $y = h_y^t(x)$ uniquely maps each input $x$ to a single label $y$. This excludes cases with label noise (Frénay & Verleysen, 2013), inherent ambiguity (e.g., subjective annotations), or stochastic data-generating processes. Extensions to probabilistic labeling functions $P(y|x)$ are left for future work.

[3]Although this analysis is focused on classification tasks, a similar derivation can be performed for regression tasks with MSE loss.

and $\mathbb{M}_t$ both cover the new and past task domains, we assume $\mathcal{L}_{\mathbb{D}_t}(h^*_{\mathbb{M}_t}, h^*_{\mathbb{D}_t})$ to be reasonably small and thus the bound is primarily driven by $\text{disc}_L(\mathbb{D}_t, \mathbb{M}_t)$.

**Remarks**. Theorem 1 highlights that a key factor influencing generalization performance is the discrepancy $\text{disc}_L(\mathbb{D}_t, \mathbb{M}_t)$, which measures the distribution difference between the stored data and the data stream. While much research focuses on constructing representative exemplars (the long-term memory), the role of the incoming buffer (short-term memory) is often overlooked (Peng et al., 2023; Ye & Bors, 2022). Theorem 1 reveals that it is the joint distribution of the long-term and short-term memories, rather than the long-term memory alone, that determines the generalization bound.

We analyze the discrepancy distance $\text{disc}_L(\mathbb{D}_t, \mathbb{M}_t)$ at task boundaries in Proposition 1.

**Proposition 1.** Assume $\mathbb{D}_t^+$ denotes the probability distribution of the most recent task $\mathcal{C}_i$ and $\mathbb{D}_t^-$ denotes the probability distribution of all past tasks seen so far $\cup_{1,\ldots,i-1}\mathcal{C}$. Given the number of samples seen in the data stream $N_t = \sum_t |\mathcal{X}_t|$ and the number of samples seen in the previous tasks $N_t^- = \sum_{k=1}^{k=i-1} |\mathcal{C}_k|$, we have:

$$\text{disc}_L(\mathbb{D}_t, \mathbb{M}_t) = \frac{N_t^- \lambda (N_t - M)}{N_t (N_t + \lambda N_t - \lambda M)} \text{disc}_L(\mathbb{D}_t^-, \mathbb{D}_t^+). \tag{3}$$

The proof is based on the property of reservoir sampling Vitter (1985) and is shown in Appendix A.2. Proposition 1 reveals the effect of $\lambda$, problem structure, and task similarity, on the discrepancy distance.

Based on Eq 9, we quantitatively compute the effect of MCR as:

**Corollary 1**.

$$\nabla_\lambda \text{disc}_L = \frac{N_t^- (N_t - M)}{(N_t + \lambda N_t - \lambda M)^2} \text{disc}_L(\mathbb{D}_t^-, \mathbb{D}_t^+) \tag{4}$$

Equation 4 reveals several insights:

1. The effect of the MCR $\lambda$: When $N_t > M$ and $\text{disc}_L(\mathbb{P}_t^-, \mathbb{P}_t^+) \neq 0$, we have $\nabla_\lambda \text{disc}_L > 0$. This suggests a smaller $\lambda$ leads to a lower discrepancy distance and a lower generalization bound.

2. Bounded vs. unbounded memory: In the case of $N_t = M$, i.e., an unbounded memory system for learning data streams, we have $\nabla_\lambda \text{disc}_L = 0$. In this case, the choice of MCR does not affect the generalization bound. A related result is $\frac{\partial^2 \text{disc}_L}{\partial N \partial \lambda} > 0$ and $\frac{\partial^2 \text{disc}_L}{\partial M \partial \lambda} < 0$. This suggests the effect of MCR becomes more evident with a longer data stream $N_t$ and a more limited memory budget $M$.

3. Task similarity: The effect of MCR also depends on task similarity $\mathbb{P}_t^-$ and $\mathbb{P}_t^+$, and the loss function $L$. With smaller $\text{disc}_L(\mathbb{P}_t^-, \mathbb{P}_t^+)$, the effect of MCR diminishes.

## 5 Empirical study on forgetting mitigation strategies and training dynamics

While our previous analysis of MCR's effect on generalization bounds reveals important theoretical insights about the relationships between MCR, task similarity, and problem structure, several key limitations remain unaddressed.

**Forgetting mitigation losses.** The generalization bound analysis assumes symmetric loss functions. However, modern continual learning methods typically employ complex asymmetric loss functions (e.g., cross-entropy and contrastive losses) with some auxiliary loss designs, like regularization loss terms based on knowledge distillation. It is unclear how these forgetting mitigation strategies interplay with the long-term and short-term allocation mechanisms. Intuitively, the incorporation of forgetting mitigation loss may reduce the necessary size of long-term memory.

**Training dynamics.** In addition, the theoretical framework of generalization bounds primarily examines relationships between model complexity, sample size, and generalization error, without explicitly considering training dynamics, such as the effects of SGD optimization and model initialization. This limitation is especially relevant to continual learning, where model initialization plays a fundamental role: at the start of each new task, the model has already been optimized for previous tasks. This creates an initial state where

the model performs well on data stored in long-term memory but poorly on new data in short-term memory. This performance disparity at initialization may also reduce the necessary size of long-term memory and thus influence the effect of the MCR.

To address these limitations, we investigate the effect of the MCR empirically, by considering practical CL training dynamics and forgetting mitigation strategies. We investigate whether the previous theoretical results hold with complex loss functions and training dynamics.

**Control Variables**. To isolate the effect of the MCR, we consider the following control factors in our empirical study:

- *Stored Data Size (M)*: We compare the effect of the MCR under a fixed total memory budget $M$. This ensures the training data size used in each model update session is consistent and eliminates potential confounding factors related to the training data size.
- *Seen Data Size (N)*: We assume that all samples of the incoming batch will be fitted in the short-term memory, i.e., $M_{short} \geq B$. This guarantees that all samples in the data stream will be used by the model at some stage, regardless of MCR value.
- *Compute Resources (K)*: We control the number of iterations to be the same when comparing the effect of the MCR. This ensures a fair comparison of the computational resources utilized across different experimental conditions.
- *Algorithms and Hyperparameters*: We compare the effect of the MCR under the exact same CL algorithms, using the same data augmentation techniques and hyperparameter settings. This allows for an isolated evaluation of the impact of the MCR.

### 5.1 Experiment setup

**Image classification**. The main experiments involve three standard CL benchmarks based on image classification: Split-CIFAR100 with 20 tasks, Split-Mini-ImageNet Vinyals et al. (2016) with 10 tasks, and CORE50 Lomonaco & Maltoni (2017) with 9 tasks. Table 1 lists the image size, the number of classes, the number of tasks, and data size per task for the four CL benchmarks. The task size in these three benchmarks is 2500, 5000, and 12000 respectively. We consider the data stream batch size to be 50. We use ResNet-18 for all experiments. We apply standard data augmentation (random cropping and flipping) in most experiments. For SCR and CORE50, we additionally use color jittering and random grayscale conversion. Hyperparameter details can be found in the Appendix D.

Table 1: Dataset information for the the three image classification benchmarks.

| | Image Size | #Task | # Class | Train per task | Test per task |
|---|---|---|---|---|---|
| Split-CIFAR100 | 3x32x32 | 20 | 100 | 2,500 | 250 |
| Split-MINI-ImageNet | 3x84x84 | 10 | 100 | 5,000 | 1,000 |
| Split-CORE50-NC | 3x128x128 | 9 | 50 | 12,000 | 4,500 |

**Text classification**. We also consider continual text classification with five text classification datasets, including AG News (news classification), Yelp (sentiment analysis), and Yahoo! Answer (Q&A classification). A summary of the text datasets is shown in Table 2.

Following (de Masson D'Autume et al., 2019; Huang et al., 2021), we utilize the pretrained BERT-base-uncased model from the HuggingFace Transformers Wolf et al. (2020) library as the base feature extractor. The experiments are conducted with a batch size of 8. The learning rate is set to 3e-5 and the weight decay for all parameters is set to 0.01.

**Evaluation metric**. The performance of CL is measured by the final accuracy after training on all tasks, defined as $A_T = \frac{1}{T}\sum_{j=1}^{j=T} a_{T,j}$, where $a_{i,j}$ denotes the model's accuracy on the held-out test set of task $j$

Table 2: Dataset information for continual learning for text classification.

| Order | Dataset | Type | #Class | Train | Test |
|---|---|---|---|---|---|
| 1 | AGNews | News | 4 | 8000 | 7600 |
| 2 | Yelp | Sentiment | 5 | 8000 | 7600 |
| 3 | Yahoo | Q&A | 10 | 20000 | 7600 |

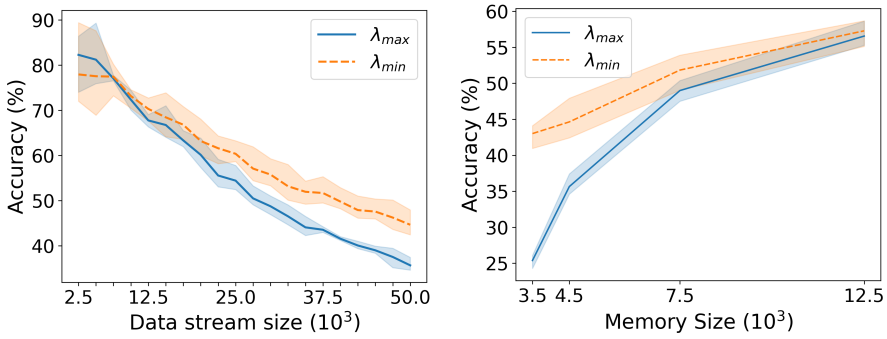


(a) Data stream size N (b) Exemplar budget M

Figure 2: Memory Capacity Ratio (MCR) and problem structure: the effect of MCR on continual learning efficacy becomes more evident with a longer data stream sequence $N$, and a smaller exemplar budget $M$. This experiment employs ER in CIFAR100 with 20 tasks.

after training on task $i$. We conduct all experiments across three random seeds to account for potential variability factors, including task splitting in continual learning benchmarks, random sample selection in reservoir sampling, random model initialization and stochastic gradient descent. The plots are presented with 95% confidence intervals to provide a measure of statistical significance. Furthermore, the tables report the mean values along with the corresponding standard deviations.

**Replay Strategies**. We consider three types of replay-based approaches: 1) *Direct rehearsal*. Our main experiment is focused on experience replay Chaudhry et al. (2019), which is a simple approach that achieves competitive performance especially in large-scale settings Prabhu et al. (2023). ER incorporates past exemplars directly in the training via cross-entropy loss. 2) *Knowledge distillation*. Many replay-based methods leverage knowledge distillation to construct a regularization loss, using a past model as the teacher and the current model as the student (Li & Hoiem, 2017; Rebuffi et al., 2017; Buzzega et al., 2020; Hinton et al., 2015). A classic method is iCaRL which maintains a past model and computes distillation loss based on the past network's outputs related to old classes. Instead of computing logits based on a past model, the distillation loss of DER++ uses the network's logits sampled throughout the optimization trajectory, and the distillation loss is computed over past exemplars. 3) *Contrastive replay*. Some recent works (Cha et al., 2021; Mai et al., 2021; Khosla et al., 2020) investigate the use of self-supervised learning techniques to learn a strong representation to reduce forgetting. A representative method is SCR Mai et al. (2021), which replaces cross-entropy with contrastive loss to capture more information about exemplars and achieves state-of-the-art performance.

**Memory and Compute**. To make the experiment results comparable to existing work, we follow the standard practice in the offline continual learning literature. We set the total memory budget to be task size plus 2000. More specifically, the total memory budget is 4500, 7000 and 14000 for CIFAR100, Mini-Imagenet and CORE50 respectively. With this setup, the results obtained with $\lambda_{max}$ are aligned with the existing offline continual learning results that employ a 2000 exemplar budget. Regarding the computational resources, we employ 50 training epochs ($K = 50$) as the default setting.

Table 3: The effect of memory capacity ratio in different benchmarks and algorithms. Given a memory budget $M$, and a data stream with task size $C$ and batch size $B$, small MCR $\lambda_{min} = B/(M-B)$ values lead to a significant performance advantage over large MCR values $\lambda_{max} = C/(M-C)$.

| | MCR | ER | iCARL | DER++ | SCR |
|---|---|---|---|---|---|
| S-CIFAR100-20 | $\lambda_{max}$ | 35.1 ± 0.8 | 44.8 ± 1.1 | 47.2 ± 0.4 | 45.1 ± 0.4 |
| | $\lambda_{min}$ | 44.6 ± 2.4 | 50.0 ± 1.6 | 50.9 ± 0.9 | 51.9 ± 0.5 |
| | | 9.5 ↑ | 5.2 ↑ | 3.7↑ | 6.8 ↑ |
| S-Mini-imagenet-10 | $\lambda_{max}$ | 31.2 ± 1.1 | 42.5 ± 1.2 | 41.0 ± 2.7 | 46.3 ± 0.4 |
| | $\lambda_{min}$ | 43.7 ± 1.2 | 46.8 ± 1.5 | 46.4 ± 1.3 | 51.8 ± 0.7 |
| | | 12.5 ↑ | 3.3 ↑ | 5.4 ↑ | 5.5↑ |
| S-CORE-9 | $\lambda_{max}$ | 40.1 ± 2.4 | 45.8 ± 1.6 | 38.2 ± 1.5 | 62.1 ± 1.3 |
| | $\lambda_{min}$ | 50.7 ± 1.7 | 50.1 ± 1.6 | 46.7 ± 2.6 | 69.7 ± 0.3 |
| | | 10.6 ↑ | 4.3 ↑ | 8.5 ↑ | 7.6 |

Table 4: The effect of memory capacity ratio $\lambda$ in task-incremental, domain-incremental and pretrained class-incremental settings.

| CL Settings | Task-Incremental | Domain-Incremental | Pretrained ResNet | Pretrained Transformer |
|---|---|---|---|---|
| Dataset | CIFAR100 | CLRS | Mini-ImageNet | Text classification |
| $\lambda_{max}$ | **83.4 ± 1.3** | 34.2 ± 2.6 | 36.6 ± 0.9 | 65.8 ± 0.5 |
| $\lambda_{min}$ | 83.1 ± 2.3 | **36.8 ± 1.3** | **48.3 ± 1.1** | **71.9 ± 0.3** |

### 5.2 Main findings

**Forgetting-mitigation strategies**. Different replay techniques make use of exemplars to preserve past knowledge in different ways. Intuitively, a replay method with a very strong forgetting mitigation design may not need a large number of exemplars from previous tasks to perform well. Thus, one interesting question is how the effect of the MCR changes with different forgetting designs. Fig 1 presents the results of different CL strategies on Split-Mini-ImageNet. Interestingly, our results show that a small MCR $\lambda$ seems to lead to better performance across different algorithms including ER, iCaRL, DER++, and SCR. The performance boost in direct rehearsal ER seems larger than in other replay methods. Table 3 presents detailed results comparing the results of the smallest MCR $\lambda_{min}$ and the largest $\lambda_{max}$ on three standard CL benchmarks. $\lambda_{min}$ leads to consistent performance improvement over $\lambda_{min}$ across three datasets (ER: $10-12\%$, iCaRL: $4-6\%$, DER++: $3-8\%$, SCR: $5-7\%$).

**Continual learning problem structure**. We further investigate whether the effect of MCR is influenced by different problem structures along two dimensions: 1) *Data stream size* - Fig 2 a) suggests that with longer task sequences the advantage of small MCR becomes more obvious. 2) *Memory budget* - Fig 2 b) presents results of different sizes of memory budget, including 3500, 4500, 7500, and 12500. Given the limited memory budget, the advantage of a small MCR is more evident. When the budget is larger than 12500 (around 5 tasks), the performance of replay remains the same regardless of the choice of MCR.

**Different CL settings.** So far, our experiments focused on the class-incremental setting and training the model from scratch. We now investigate this phenomenon in other settings. The effect of the MCR $\lambda$ in task-incremental (TI), domain-incremental (DI) and pretrained class-incremental settings is shown in Table 4. When initializing the model with a pre-trained ResNet18, we observe a similar trend: ER with a small MCR ($48.3 \pm 1.1\%$) significantly outperforms ER with large MCR values ($36.6 \pm 0.9\%$). Additionally to what is observed with ResNet and image data, we also observe similar results in text classification experiments with pre-trained Transformer models ($\lambda_{min}$ : $71.9 \pm 0.3\%$ and $\lambda_{max}$ : $65.8 \pm 0.3\%$). However, in task-incremental learning, we observe the effect of the MCR ratio is not significant ($\lambda_{min}$ : $83.1 \pm 2.3\%$ and $\lambda_{max}$ : $83.4 \pm 1.3\%$).

Table 5: The effect of MCR on different sample selection methods, including MIR and ASER.

| Method | MCR | Mini-ImageNet | | CIFAR-100 | |
|---|---|---|---|---|---|
| | | $M_{short}$ | Accuracy | $M_{short}$ | Accuracy |
| MIR | $\lambda_{min}$ | 50 | $\mathbf{43.4 \pm 0.3}$ | 50 | $\mathbf{43.4 \pm 3.1}$ |
| | $\lambda_{mid}$ | 2500 | $40.6 \pm 0.5$ | 1250 | $41.4 \pm 1.4$ |
| | $\lambda_{max}$ | 5000 | $30.8 \pm 0.6$ | 2500 | $33.4 \pm 2.8$ |
| ASER | $\lambda_{min}$ | 50 | $\mathbf{40.6 \pm 0.8}$ | 50 | $\mathbf{42.8 \pm 1.7}$ |
| | $\lambda_{mid}$ | 2500 | $38.2 \pm 0.6$ | 1250 | $41.0 \pm 2.2$ |
| | $\lambda_{max}$ | 5000 | $31.1 \pm 1.0$ | 2500 | $33.8 \pm 1.2$ |

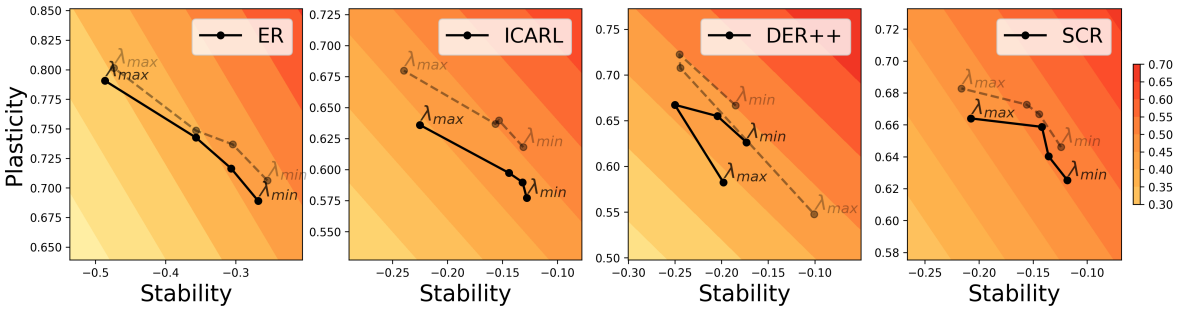


Figure 3: Stability, plasticity, and generalization across two runs with different initializations and task splits. Reducing MCR yields three stability–plasticity patterns: (1) ↑stability ↓plasticity, (2) ↑stability ↑plasticity, and (3) ↓stability ↑plasticity.

**Memory Management Policies**. Table 5 presents results using different memory update and retrieval strategies, including MIR (Aljundi et al., 2019) and ASER (Shim et al., 2021). Unlike random selection, MIR retrieves samples that are most interfered—i.e., those whose predictions would be most negatively affected by upcoming parameter updates. ASER, on the other hand, selects samples based on the Adversarial Shapley value, which scores memory samples by their contribution to preserving latent decision boundaries of previously observed classes. Consistent with our main findings, Table 5 shows that reducing MCR also improves performance when using advanced sample selection methods such as MIR and ASER.

In summary, our empirical study reveals that the relative capacity of long-term and short-term memory exhibits a complex interplay with forgetting-mitigation strategies and problem structure. For certain problems, such as task-incremental learning or scenarios with a large memory budget, the choice of MCR does not significantly impact performance. However, in other settings like class-incremental learning with a limited memory budget, the performance of replay methods can be significantly improved by adopting smaller MCR values. To understand how MCR influences the learning efficacy of continual learning systems, we examine the stability and plasticity dynamics next.

## 6 Stability and Plasticity

**Measuring stability and plasticity**. Beyond the evaluation of the overall performance as discussed in Section 5.1, we also examine the stability and plasticity during the learning process. Plasticity refers to the ability to learn the new tasks and is usually measured as the accuracy on the new task. Stability refers to the ability to maintain previous knowledge. There are two measures proposed in the literature related to stability: one metric is "forgetting" (Chaudhry et al., 2018), which is defined as $F_T = -\frac{1}{T-1}\sum_{i=1}^{T-1}(a_{T,i} - \max_{l\in 1\ldots T-1} a_{l,i})$ and the related metric "backward transfer" (Lopez-Paz & Ranzato, 2017): $B_T = \frac{1}{T-1}\sum_{i=1}^{T-1} a_{T,i} - a_{i,i}$. Since

the continual learning systems require a tradeoff of stability and plasticity, Zhang et al. (2022) decompose the overall CL performance into a stability-based term and a plasticity-based term, as follows:

$$A_T = \underbrace{\frac{1}{T}\Sigma_{i=1}^{T} a_{i,i}}_{\text{Plasticity}} + \underbrace{\frac{T-1}{T} B_T}_{\text{Stability}} \geq \frac{1}{T}\Sigma_{i=1}^{T} a_{i,i} - \frac{T-1}{T} F_T.$$

**Insights into Stability-Plasticity Dynamics**. Using the definitions of stability, plasticity, and generalization from Zhang et al. (2022), we plot the effect of the MCR on these metrics in Fig 3. Since a lower MCR allocates more space for storing past exemplars and less space for new samples from the current task, an intuitive expectation would be that reducing the MCR leads to better stability and worse plasticity. Surprisingly, this behavior is observed only in some algorithms (ER, iCaRL, and SCR). For other algorithms (e.g., DER++), reducing MCR leads to various types of stability-plasticity behaviors, including better plasticity and better stability at some stages, and better plasticity and worse stability at other stages, as shown in Fig. 3. These behaviors in DER++ suggest that increasing the ratio of long-term memory can aid in the learning of new tasks at certain stages.

To understand why increasing long-term memory can contribute to plasticity in some cases, we consider the distribution composition of long-term buffers. The long-term memory contains a subset of past data, and its coverage is determined by where the data stream is split. As illustrated in Fig 1, the data stream is split into two parts based on the size of the short-term memory ($M_{short}$): one part contains the recent $M_{short}$ samples, which are greedily stored in the short-term memory, and the other part contains all the samples before $M_{short}$, which are selectively captured by the long-term memory. With reservoir sampling, the long-term memory stores a fraction $p_{new}$ of new task exemplars and $1 - p_{new}$ of old task exemplars: $p_{new} = \frac{C - M_{short}}{N - M_{short}}$, where $N$ is the data stream size and $C$ is the task size. When $M_{short} < C$ (i.e., in online and semi-offline CL), we have $p_{new} > 0$, meaning the long-term memory contributes to learning the current task, promoting plasticity. We take DER as an example to illustrate how the MCR may lead to complex stability-plasticity changes. The analysis of other algorithms follows a similar manner and can be found in Appendix C. We rewrite the gradient of DER as follows:

$$\begin{aligned} \nabla \mathcal{L}_{DER} &= \mathbb{E}_{\mathcal{M}_{short}}[\nabla \ell_{ce}] + \mathbb{E}_{\mathcal{M}_{long}}[\nabla \ell_{mse}^{kd}] \\ &= \mathbb{E}_{\mathcal{M}_{short}}[\nabla \ell_{ce}] + p_{new} \times \mathbb{E}_{\mathcal{M}_{long}^{new}}[\nabla \ell_{mse}^{kd}] + (1 - p_{new}) \times \mathbb{E}_{\mathcal{M}_{long}^{old}}[\nabla \ell_{mse}^{kd}] \end{aligned} \tag{5}$$

As shown in Eq 5, when the ratio of short-term memory is reduced, the first term of the right-hand side (RHS) suffers from greater overfitting of new task data, which harms plasticity. However, the second term of the RHS drives plasticity, and its contribution increases with smaller $M_{short}$ because $\nabla_{M_{short}} p_{new} < 0$. Therefore, the overall plasticity is determined by the interplay between the first and second terms. DER employs different loss functions for the first term (cross-entropy) and second term (logits-based knowledge distillation), thus creating the complex plasticity dynamics in Fig 3.

## 7 Discussion and Conclusion

A key challenge in continual learning is optimizing memory usage to enhance learning efficiency. While many prior works have investigated different strategies for selecting and storing representative past data, the higher-level memory architecture governing the interaction between old and new data remains understudied. In this work, we identify and formalize a unified dual-memory system that naturally arises in both online and offline CL settings. This system comprises: (1) short-term memory, which temporarily buffers recent data for immediate model updates, and (2) long-term memory, which maintains a carefully curated subset of past experiences for future replay and consolidation. We investigate how the memory capacity ratio (MCR), defined as the relative allocation of resources between STM and LTM, affects learning efficacy in non-stationary streams. Empirically, we find that reducing the MCR induces distinct stability-plasticity trade-offs depending on the replay mechanism: some replay configurations improve both stability and plasticity, others enhance one at the expense of the other, yet a smaller MCR consistently matches or outperforms larger MCRs in

generalization. Theoretical analysis of generalization bounds in a simplified setting further supports this result.

We believe the impact of MCR has likely remained unexplored in prior work because 1) CL memory is often treated as a monolithic store of exemplars, and 2) online/offline CL are typically studied in isolation with divergent setups. By re-examining continual replay through the lens of short- and long-term memory, our work offers a more comprehensive understanding of replay dynamics in non-stationary environments. Our findings suggest that designing a memory structure with a small MCR can be advantageous in building practical continual learning systems, such as those used in affective robotics (Churamani et al., 2020), smart home assistants, or wearable devices.

**Limitations.** This work examines rehearsal and knowledge distillation techniques for continual learning. Other approaches, such as correcting task recency bias (Wu et al., 2019; Hou et al., 2019) or expanding network capacity (Zhou et al., 2022; Yan et al., 2021), are not covered by our analysis. Additionally, we use a fixed MCR throughout the continual learning process. Since MCR directly influences the trade-off between stability and plasticity, dynamically adjusting MCR to achieve a better balance between the two represents a promising direction for future research. Moreover, with a time-varying MCR, an interesting avenue for exploration is designing an adaptive memory management strategy that aligns with the changing memory size while maintaining representativeness across different tasks.

## References

Rahaf Aljundi, Eugene Belilovsky, Tinne Tuytelaars, Laurent Charlin, Massimo Caccia, Min Lin, and Lucas Page-Caccia. Online continual learning with maximal interfered retrieval. *Advances in Neural Information Processing Systems*, 32:11849–11860, 2019.

Shai Ben-David and Ruth Urner. The sample complexity of agnostic learning under deterministic labels. In *Conference on Learning Theory*, pp. 527–542. PMLR, 2014.

Pietro Buzzega, Matteo Boschini, Angelo Porrello, Davide Abati, and Simone Calderara. Dark experience for general continual learning: a strong, simple baseline. *Advances in neural information processing systems*, 33:15920–15930, 2020.

Lucas Caccia, Rahaf Aljundi, Nader Asadi, Tinne Tuytelaars, Joelle Pineau, and Eugene Belilovsky. New insights on reducing abrupt representation change in online continual learning. In *International Conference on Learning Representations*, 2021.

Francisco M Castro, Manuel J Marín-Jiménez, Nicolás Guil, Cordelia Schmid, and Karteek Alahari. End-to-end incremental learning. In *Proceedings of the European conference on computer vision (ECCV)*, pp. 233–248, 2018.

Hyuntak Cha, Jaeho Lee, and Jinwoo Shin. Co2L: Contrastive continual learning. In *Proceedings of the IEEE/CVF International Conference on Computer Vision*, pp. 9516–9525, 2021.

Arslan Chaudhry, Marc'Aurelio Ranzato, Marcus Rohrbach, and Mohamed Elhoseiny. Efficient lifelong learning with a-gem. In *International Conference on Learning Representations*, 2018.

Arslan Chaudhry, Marcus Rohrbach, Mohamed Elhoseiny, Thalaiyasingam Ajanthan, Puneet K Dokania, Philip HS Torr, and Marc'Aurelio Ranzato. On tiny episodic memories in continual learning. *arXiv preprint arXiv:1902.10486*, 2019.

Aristotelis Chrysakis and Marie-Francine Moens. Online bias correction for task-free continual learning. *ICLR 2023 at OpenReview*, 2023.

Nikhil Churamani, Sinan Kalkan, and Hatice Gunes. Continual learning for affective robotics: Why, what and how? In *2020 29th IEEE international conference on robot and human interactive communication (RO-MAN)*, pp. 425–431. IEEE, 2020.

Cyprien de Masson D'Autume, Sebastian Ruder, Lingpeng Kong, and Dani Yogatama. Episodic memory in lifelong language learning. *Advances in Neural Information Processing Systems*, 32, 2019.

Matthias Delange, Rahaf Aljundi, Marc Masana, Sarah Parisot, Xu Jia, Ales Leonardis, Greg Slabaugh, and Tinne Tuytelaars. A continual learning survey: Defying forgetting in classification tasks. *IEEE Transactions on Pattern Analysis and Machine Intelligence*, 2021.

Thang Doan, Mehdi Abbana Bennani, Bogdan Mazoure, Guillaume Rabusseau, and Pierre Alquier. A theoretical analysis of catastrophic forgetting through the ntk overlap matrix. In *International Conference on Artificial Intelligence and Statistics*, pp. 1072–1080. PMLR, 2021.

Benoît Frénay and Michel Verleysen. Classification in the presence of label noise: a survey. *IEEE transactions on neural networks and learning systems*, 25(5):845–869, 2013.

Geoffrey Hinton, Oriol Vinyals, and Jeff Dean. Distilling the knowledge in a neural network. *arXiv preprint arXiv:1503.02531*, 2015.

Saihui Hou, Xinyu Pan, Chen Change Loy, Zilei Wang, and Dahua Lin. Learning a unified classifier incrementally via rebalancing. In *Proceedings of the IEEE/CVF conference on computer vision and pattern recognition*, pp. 831–839, 2019.

Yufan Huang, Yanzhe Zhang, Jiaao Chen, Xuezhi Wang, and Diyi Yang. Continual learning for text classification with information disentanglement based regularization. In *Proceedings of the 2021 Conference of the North American Chapter of the Association for Computational Linguistics: Human Language Technologies*, pp. 2736–2746, 2021.

Dahuin Jung, Dongjin Lee, Sunwon Hong, Hyemi Jang, Ho Bae, and Sungroh Yoon. New insights for the stability-plasticity dilemma in online continual learning. In *The Eleventh International Conference on Learning Representations*, 2022.

Prannay Khosla, Piotr Teterwak, Chen Wang, Aaron Sarna, Yonglong Tian, Phillip Isola, Aaron Maschinot, Ce Liu, and Dilip Krishnan. Supervised contrastive learning. *Advances in neural information processing systems*, 33:18661–18673, 2020.

Z Li and D Hoiem. Learning without forgetting. *IEEE Transactions on Pattern Analysis and Machine Intelligence*, 40(12):2935–2947, 2017.

Vincenzo Lomonaco and Davide Maltoni. CORe50: a new dataset and benchmark for continuous object recognition. In *Conference on Robot Learning*, pp. 17–26. PMLR, 2017.

David Lopez-Paz and Marc'Aurelio Ranzato. Gradient episodic memory for continual learning. *Advances in neural information processing systems*, 30, 2017.

Zheda Mai, Ruiwen Li, Hyunwoo Kim, and Scott Sanner. Supervised contrastive replay: Revisiting the nearest class mean classifier in online class-incremental continual learning. In *Proceedings of the IEEE/CVF Conference on Computer Vision and Pattern Recognition*, pp. 3589–3599, 2021.

Zheda Mai, Ruiwen Li, Jihwan Jeong, David Quispe, Hyunwoo Kim, and Scott Sanner. Online continual learning in image classification: An empirical survey. *Neurocomputing*, 469:28–51, 2022.

Arun Mallya and Svetlana Lazebnik. Packnet: Adding multiple tasks to a single network by iterative pruning. In *Proceedings of the IEEE conference on Computer Vision and Pattern Recognition*, pp. 7765–7773, 2018.

Yishay Mansour, Mehryar Mohri, and Afshin Rostamizadeh. Domain adaptation: Learning bounds and algorithms. In *The 22nd Conference on Learning Theory*, 2009. URL `http://www.cs.mcgill.ca/%7Ecolt2009/papers/003.pdf#page=1`.

Marc Masana, Xialei Liu, Bartłomiej Twardowski, Mikel Menta, Andrew D Bagdanov, and Joost Van De Weijer. Class-incremental learning: survey and performance evaluation on image classification. *IEEE Transactions on Pattern Analysis and Machine Intelligence*, 45(5):5513–5533, 2022.

M Jehanzeb Mirza, Marc Masana, Horst Possegger, and Horst Bischof. An efficient domain-incremental learning approach to drive in all weather conditions. In *Proceedings of the IEEE/CVF Conference on Computer Vision and Pattern Recognition*, pp. 3001–3011, 2022.

Liangzu Peng, Paris Giampouras, and René Vidal. The ideal continual learner: An agent that never forgets. In *International Conference on Machine Learning*, pp. 27585–27610. PMLR, 2023.

Ameya Prabhu, Hasan Abed Al Kader Hammoud, Puneet K Dokania, Philip HS Torr, Ser-Nam Lim, Bernard Ghanem, and Adel Bibi. Computationally budgeted continual learning: What does matter? In *Proceedings of the IEEE/CVF Conference on Computer Vision and Pattern Recognition*, pp. 3698–3707, 2023.

Sylvestre-Alvise Rebuffi, Alexander Kolesnikov, Georg Sperl, and Christoph H Lampert. iCaRL: Incremental classifier and representation learning. In *Proceedings of the IEEE conference on Computer Vision and Pattern Recognition*, pp. 2001–2010, 2017.

Joan Serra, Didac Suris, Marius Miron, and Alexandros Karatzoglou. Overcoming catastrophic forgetting with hard attention to the task. In *International conference on machine learning*, pp. 4548–4557. PMLR, 2018.

Dongsub Shim, Zheda Mai, Jihwan Jeong, Scott Sanner, Hyunwoo Kim, and Jongseong Jang. Online class-incremental continual learning with adversarial shapley value. In *Proceedings of the AAAI Conference on Artificial Intelligence*, volume 35, pp. 9630–9638, 2021.

Albin Soutif-Cormerais, Antonio Carta, Andrea Cossu, Julio Hurtado, Vincenzo Lomonaco, Joost Van de Weijer, and Hamed Hemati. A comprehensive empirical evaluation on online continual learning. In *Proceedings of the IEEE/CVF International Conference on Computer Vision*, pp. 3518–3528, 2023.

Gido M Van de Ven and Andreas S Tolias. Three scenarios for continual learning. *NeurIPS - Continual Learning workshop*, 2019.

Oriol Vinyals, Charles Blundell, Timothy Lillicrap, and Daan Wierstra. Matching networks for one shot learning. *Advances in neural information processing systems*, 29:3630–3638, 2016.

Jeffrey S Vitter. Random sampling with a reservoir. *ACM Transactions on Mathematical Software (TOMS)*, 11(1):37–57, 1985.

Thomas Wolf, Lysandre Debut, Victor Sanh, Julien Chaumond, Clement Delangue, Anthony Moi, Pierric Cistac, Tim Rault, Remi Louf, Morgan Funtowicz, Joe Davison, Sam Shleifer, Patrick von Platen, Clara Ma, Yacine Jernite, Julien Plu, Canwen Xu, Teven Le Scao, Sylvain Gugger, Mariama Drame, Quentin Lhoest, and Alexander Rush. Transformers: State-of-the-art natural language processing. In Qun Liu and David Schlangen (eds.), *Proceedings of the 2020 Conference on Empirical Methods in Natural Language Processing: System Demonstrations*, pp. 38–45, Online, October 2020. Association for Computational Linguistics. doi: 10.18653/v1/2020.emnlp-demos.6. URL `https://aclanthology.org/2020.emnlp-demos.6`.

Yue Wu, Yinpeng Chen, Lijuan Wang, Yuancheng Ye, Zicheng Liu, Yandong Guo, and Yun Fu. Large scale incremental learning. In *Proceedings of the IEEE/CVF Conference on Computer Vision and Pattern Recognition*, pp. 374–382, 2019.

Shipeng Yan, Jiangwei Xie, and Xuming He. Der: Dynamically expandable representation for class incremental learning. In *Proceedings of the IEEE/CVF Conference on Computer Vision and Pattern Recognition*, pp. 3014–3023, 2021.

Fei Ye and Adrian G Bors. Task-free continual learning via online discrepancy distance learning. *Advances in Neural Information Processing Systems*, 35:23675–23688, 2022.

Yaqian Zhang, Bernhard Pfahringer, Eibe Frank, Albert Bifet, Nick Jin Sean Lim, and Yunzhe Jia. A simple but strong baseline for online continual learning: Repeated augmented rehearsal. *Advances in Neural Information Processing Systems*, 35:14771–14783, 2022.

Da-Wei Zhou, Qi-Wei Wang, Han-Jia Ye, and De-Chuan Zhan. A model or 603 exemplars: Towards memory-efficient class-incremental learning. In *The Eleventh International Conference on Learning Representations*, 2022.

# A Proofs

[4]

## A.1 Proof of Theorem 1

*Proof.* We follow the derivations of Theorem 8 in Mansour et al. (2009) and Theorem 1 in Ye & Bors (2022):

$$\begin{aligned}\mathcal{L}_{\mathbb{D}}(h, h_y) &\leq \mathcal{L}_{\mathbb{D}}(h, h^*_{\mathbb{M}}) + \mathcal{L}_{\mathbb{D}}(h^*_{\mathbb{M}}, h^*_{\mathbb{D}}) + \mathcal{L}_{\mathbb{D}}(h^*_{\mathbb{D}}, h_y) \\ &\leq \mathcal{L}_{\mathbb{M}}(h, h^*_{\mathbb{M}}) + \mathrm{disc}_L(\mathbb{D}, \mathbb{M}) + \mathcal{L}_{\mathbb{D}}(h^*_{\mathbb{M}}, h^*_{\mathbb{D}}) + \mathcal{L}_{\mathbb{D}}(h^*_{\mathbb{D}}, h_y) \\ &\leq \mathcal{L}_{\hat{\mathbb{M}}}(h, h^*_{\mathbb{M}}) + \widehat{\Re}_{\mathcal{M}}(H) + 3A_0\sqrt{\frac{\log\frac{2}{\delta}}{2M}} + \mathrm{disc}_L(\mathbb{D}, \mathbb{M}) + \mathcal{L}_{\mathbb{D}}(h^*_{\mathbb{M}}, h^*_{\mathbb{D}}) + \mathcal{L}_{\mathbb{D}}(h^*_{\mathbb{D}}, h_y),\end{aligned} \tag{6}$$

The first inequality is based on the triangle inequality of $\mathcal{L}$. The second inequality is based on the definition of discrepancy distance $\mathrm{disc}_L$. The third inequality is based on the Rademacher Bound (Proposition 2 in Mansour et al. (2009)). □

## A.2 Proof of Proposition 1

*Proof.* Let $\gamma \doteq \frac{N^-}{N}$ and $\alpha \doteq \frac{M_{short}}{M}$. Based on the definition of discrepancy distance, we have:

$$\begin{aligned}&\mathrm{disc}_L(\mathbb{D}, \mathbb{M}) \\ &= \max_{h,h' \in H} |\gamma\mathcal{L}_{\mathbb{P}^-}(h', h) + (1-\gamma)\mathcal{L}_{\mathbb{P}^+}(h', h) \\ &\qquad - \big((1-\alpha)\mathcal{L}_{\mathbb{M}_{long}}(h', h) + \alpha\mathcal{L}_{\mathbb{M}_{short}}(h', h)\big)\,|.\end{aligned} \tag{7}$$

Since all the samples from the short-term memory come from the current task, $\mathcal{L}_{\mathbb{M}_{short}}(h', h)$ only depends on the current task distribution and is not affected by the size of short-term and long-term memory, i.e. we have $\mathcal{L}_{\mathbb{M}_{short}}(h', h) = \mathcal{L}_{\mathbb{P}^+}(h', h)$. In contrast, the long-term memory is managed by the reservoir sampling method and thus $\mathcal{L}_{\mathbb{M}_{long}}(h', h)$ is affected by the memory allocation factor $\lambda$. Letting $\beta \doteq \frac{N^-}{N-\alpha M}$, we have $\mathcal{L}_{\mathbb{M}_{long}}(h', h) = \beta\mathcal{L}_{\mathbb{P}^-}(h', h) + (1-\beta)\mathcal{L}_{\mathbb{P}^+}(h', h)$. Inserting these two results into Eq 7 gives:

$$\begin{aligned}&\mathrm{disc}_L(\mathbb{D}, \mathbb{M}) \\ &= \max_{h,h' \in H} |(\gamma - (1-\alpha)\beta))\,(\mathcal{L}_{\mathbb{P}^-}(h', h) - \mathcal{L}_{\mathbb{P}^+}(h', h))\,| \\ &= (\gamma - (1-\alpha)\beta)) \max_{h,h' \in H} |\,(\mathcal{L}_{\mathbb{P}^-}(h', h) - \mathcal{L}_{\mathbb{P}^+}(h', h))\,| \\ &= \frac{N^-\lambda(N-M)}{N(N+\lambda N-\lambda M)}\,\mathrm{disc}_L(\mathbb{P}_-, \mathbb{P}_+).\end{aligned} \tag{8}$$

This second equality is based on the fact that $\gamma - (1-\alpha)\beta = \frac{\alpha N^-(N-M)}{N(N-\alpha M)} > 0$ when $N > M$. The third equality is based on the definitions of $\alpha$, $\gamma$, $\beta$, $\lambda$, and $\mathrm{disc}_L$ □

[4] In the proof, we drop $t$ from the symbols for conciseness.

Table 6: The compute and data storage cost of online and offline continual learning on the same CL benchmark Split-CIFAR100.

| | Papers | Data Storage (# samples) | | Compute |
|---|---|---|---|---|
| | | Exemplar | New data | Iteration/Epoch |
| online CL | ER Chaudhry et al. (2019) | 2000, 5000 | 10 | 1 |
| | ER-ACE Caccia et al. (2021) | | | 1 |
| | SCR (Mai et al., 2021) | | | 1 |
| | ER-OBC (Chrysakis & Moens, 2023) | | | 1 |
| | RAR (Zhang et al., 2022) | | | 10 |
| | Survey (Mai et al., 2022) | | | 1,5 |
| | Survey (Soutif-Cormerais et al., 2023) | | | 3 |
| offline CL | ICARL Rebuffi et al. (2017) | 2000,5000 | 2500,5000 | 70 |
| | EEIL Castro et al. (2018) | | | 70 |
| | LUCIR Hou et al. (2019) | | | 160 |
| | DER++ (Buzzega et al., 2020) | | | 50 |
| | MEMO (Zhou et al., 2022) | | | 170 |
| | BIC (Wu et al., 2019) | | | 250 |
| | Survey Masana et al. (2022) | | | 100 |
| online, semi-offline, offline CL | ours | $\frac{1}{1+\lambda}M$ | $\frac{\lambda}{1+\lambda}M$ | 50 |

### A.3 Proof of Corollary 1

$$
\begin{aligned}
\nabla_\lambda \operatorname{disc}_L(\mathbb{D}_t, \mathbb{M}_t) =& \nabla_\lambda \frac{N_t^- \lambda (N_t - M)}{N_t(N_t + \lambda N_t - \lambda M)} \operatorname{disc}_L(\mathbb{D}_t^-, \mathbb{D}_t^+) \\
=& \operatorname{disc}_L(\mathbb{D}_t^-, \mathbb{D}_t^+) \frac{N_t^-(N_t - M)}{N_t} \nabla_\lambda \frac{\lambda}{N_t + \lambda N_t - \lambda M} \\
=& \operatorname{disc}_L(\mathbb{D}_t^-, \mathbb{D}_t^+) \frac{N_t^-(N_t - M)}{N_t} \nabla_\lambda \frac{1}{\frac{N_t}{\lambda} + N_t - M} \\
=& \operatorname{disc}_L(\mathbb{D}_t^-, \mathbb{D}_t^+) \frac{N_t^-(N_t - M)}{N_t} \frac{1}{(\frac{N_t}{\lambda} + N_t - M)^2} \frac{N_t}{\lambda^2} \\
=& \frac{N_t^-(N_t - M)}{(N_t + \lambda N_t - \lambda M)^2} \operatorname{disc}_L(\mathbb{D}_t^-, \mathbb{D}_t^+)
\end{aligned}
\tag{9}
$$

## B A review of memory and compute setups in continual learning

Online and offline CL are typically studied separately with different memory and compute setups (see Table B). For the compute cost, offline CL papers and surveys typically utilize 50-250 training epochs on standard benchmarks, while online CL by design can only use a single epoch. Moreover, while the gradient update steps in online CL can be increased by using repeated iteration, conducting multiple gradient updates for each incoming batch (Zhang et al., 2022; Soutif-Cormerais et al., 2023), the number of iterations is commonly chosen to be less than 10. For the storage cost, a common practice in CL is comparing different online or offline CL methods based on a fixed budget of exemplars—a subset of past samples. Less discussed is the sample complexity and storage cost introduced by the new task data, which also occupies the constrained space and is used for the training. At each training session, offline CL needs to store the full task datasets for model training, whereas online CL only stores the most recent incoming batches of the new task.

## C Stability and plasticity analysis

As shown in Section 6, in DER, the new data and exemplar data use different loss functions. In ER, SCR, and iCaRL, the two employ the same type of loss function. The gradients can be rewritten as follows:

$$\begin{aligned}\nabla\mathcal{L} &= \mathbb{E}_{\mathcal{M}_{short}}[\nabla\ell] + \mathbb{E}_{\mathcal{M}_{long}}[\nabla\ell] \\ &= \mathbb{E}_{\mathcal{M}_{short}}[\nabla\ell] + p_{new} \times \mathbb{E}_{\mathcal{M}_{long}^{new}}[\nabla\ell] + (1-p_{new}) \times \mathbb{E}_{\mathcal{M}_{long}^{old}}[\nabla\ell]\end{aligned} \tag{10}$$

Based on $p_{new} = \frac{C-M_s}{N-M_s}$, we have $p_{new} \ll 1$ in our main experiments. In particular, based on the task size and datastream sizes, we have: CIFAR100 $p_{new} \in [0, 0.045]$, Mini-ImageNet $p_{new} \in [0, 0.099]$, CORE-50 $p_{new} \in [0, 0.100]$). Thus, the plasticity changes are dominated by the first term: as the size of the short-term memory decreases, the first term faces greater overfitting on the new task data, harming plasticity. In contrast, DER++ employs different losses for the first and second terms, which leads to various plasticity dynamics as shown in Figure 3.

## D Experiment setup

**Implementation details** Our experiments were conducted on NVIDIA RTX 1080 Ti, 2080 Ti, and A6000 GPUs. In the main experiment, using a batch size of 50, each run for CIFAR100, Mini-ImageNet and CORE50 took roughly 2h, 9h, and 30h respectively. Following Masana et al. (2022), all experiments utilized ResNet-18. We use standard data augmentation (random cropping and flipping), a data stream batch size of 50 for CIFAR100 and Mini-Imagenet, 64 for CORE50. An equal number of exemplars is sampled at each gradient step. All models use vanilla SGD for optimization with a learning rate of 0.1. For iCaRL and SCR, a nearest-class-mean (NCM) classifier is applied as in the original publications. The default iteration and epoch number is 50.

**Hyperparameters**. The hyperparameter settings are summarized in Table 7. The regularization strength in DER++ and the temperature values in SCR follow the original papers.

Table 7: Hyperparameter settings.

| | Hyperparameter |
|---|---|
| ER | lr=0.1 |
| iCaRL | lr=0.1,NCM classifier |
| SCR | temp =0.07, lr=0.1, NCM classifier |
| DER ++ | $\alpha = 0.1$, $\beta = 0.5$,$lr = 0.03$ (CIFAR100) |
| | $\alpha = 0.3$ $\beta = 0.8$,$lr = 0.1$ (mini-imagenet) |
| | $\alpha = 0.1$, $\beta = 1.0$,$lr = 0.1$ (core50) |

## E Unifed continual replay framwork instantiated with DER++

Algorithm 2 integrates the DER++ method into the framework. Since DER++ uses the past logits output for knowledge distillation, the algorithm stores first the logit outputs from the learning trajectory in the short-term memory (line 17). These logits are then transferred to the long-term memory for use in future knowledge distillation steps (line 5).

## F Additional Experimental Results

The main paper shows the stability and plasticity analysis with Mini-ImageNet. Here, Fig 4 shows the results with CIFAR100 with different task numbers (20 tasks vs. 50 tasks) and across architectures (ResNet-18 and ResNet-34). These new results show behavior consistent with our previous findings. For ER, SCR, and ICARL, a smaller memory consumption ratio (MCR) leads to increased stability but decreased plasticity.

**Algorithm 2:** Unified continual replay framework instantiated with DER++

// Non-stationary data stream: $\mathcal{D}_t = \cup_t \mathcal{X}_t$, where $\mathcal{X}_t$ is the incoming batch
// Short-term memory $\mathcal{M}_{short}$: storing new data
// Long-term memory $\mathcal{M}_{long}$: storing past data
// offline CL: $|\mathcal{M}_{short}|$ is equal to the task size $|\cup_{T_i \leq t < T_{i+1}} \mathcal{X}_t|$
// online CL: $|\mathcal{M}_{short}|$ is equal to the stream batch size $|\mathcal{X}_t|$
// $\pi$ is a memory management policy
// $z$ is logits output and scalars $\alpha, \beta$ are regularization hyperparameters of DER++

**function** ContinualLearning($\mathcal{X}_t$, $\theta$, $\mathcal{M}_{short}$, $\mathcal{M}_{long}$,)
  $\mathcal{M}_{short} \leftarrow \mathcal{M}_{short} \cup \mathcal{X}_t$ // Update short-term memory
  **if** $\mathcal{M}_{short}$ is full **then**
    $\theta, \mathcal{M}_{short} \leftarrow$ ModelTraining($\theta$, $\mathcal{M}_{short}$, $\mathcal{M}_{long}$)
    $\mathcal{M}_{long} \subset_\pi \mathcal{M}_{short} \cup \mathcal{M}_{long}$ // Update long-term memory
    $\mathcal{M}_{short} \leftarrow \emptyset$
  **return** $\theta$, $\mathcal{M}_{short}$, $\mathcal{M}_{long}$
**function** ModelTraining($\theta$, $\mathcal{M}_{short}$, $\mathcal{M}_{long}$)
  **for** K epochs **do**
    **for** $\mathcal{B}_{short} = \{x, y\}$ in $\mathcal{M}_{short}$ **do**
      sample $\mathcal{B}'_{long} = \{x', y', z'_{prev}\}$ from $\mathcal{M}_{long}$,
      sample $\mathcal{B}''_{long} = \{x'', y'', z''_{prev}\}$ from $\mathcal{M}_{long}$,
      $x, x', x'' \leftarrow aug(x'), aug(x'), aug(x'')$
      $z = h_\theta(x)$
      $L_{DER++} = \ell_{ce}(x, y; \theta) + \alpha \left\| z'_{prev} - h_\theta(x') \right\|_2^2 + \beta \ell_{ce}(x'', y''; \theta)$
      $\theta \leftarrow \theta - \eta \nabla L_{DER++}$
      update $\mathcal{M}_{short}$ with logits information $\mathcal{B}_{short} = \{x, y, z\}$
  **return** $\theta, \mathcal{M}_{short}$

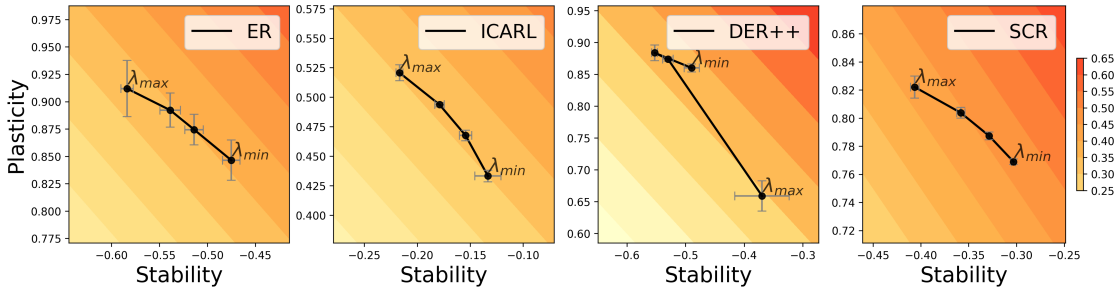


(a) ResNet-18 with 50 tasks

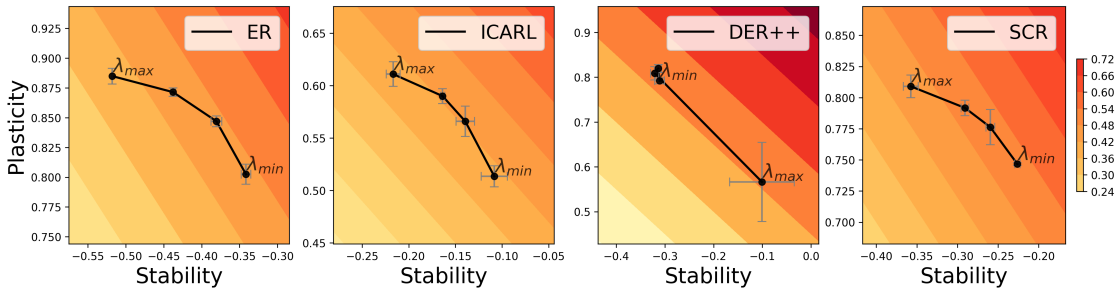


(b) ResNet-18 with 20 tasks

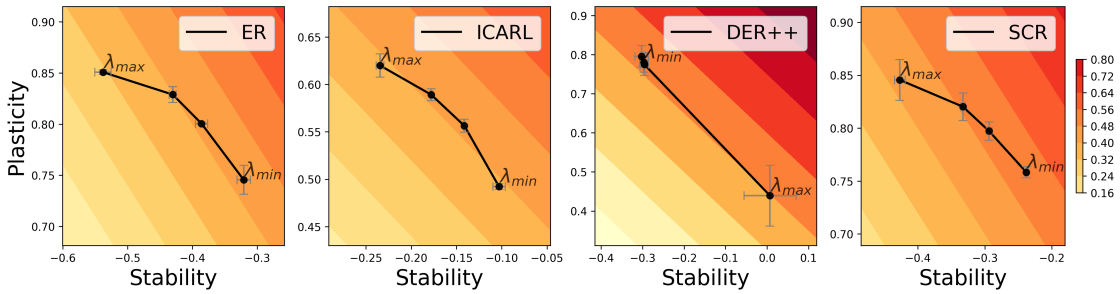


(c) ResNet-34 with 20 tasks

Figure 4: Stability and plasticity analysis with different model architectures (ResNet18 and ResNet34) and different task numbers (20 and 50 tasks) in CIFAR100.

For DER++, reducing the MCR results in different stability-plasticity behaviors, such as improved plasticity or improved stability at certain stages.